Dyes and Pigments 88 (2010) 195–203

Contents lists available at ScienceDirect

Dyes and Pigments

journal homepage: www.elsevier.com/locate/dyepig

The synthesis and spectral characterization of red dyes containing biphenyl or fluorene conjugation and dicyanovinyl acceptors

Abhishek Baheti, Prachi Singh, K.R. Justin Thomas*

Department of Chemistry, Indian Institute of Technology Roorkee, Roorkee 247 667, India

ARTICLE INFO

Article history:
Received 22 March 2010
Received in revised form
19 June 2010
Accepted 21 June 2010
Available online 1 July 2010

Keywords:
Dipolar compounds
Fluorene
Biphenyl
Red emission
Solvatochromism
Dicyanovinyl

ABSTRACT

Novel dipolar compounds containing diarylamine donors, dicyanovinyl acceptors and either a fluorene or biphenyl linker were prepared in an attempt to unravel the similarities and differences between the biphenyl and fluorene segments in donor–acceptor architectures. The linker segments significantly modify λ_{max} and the redox potential of the dyes is influenced by the nature of both the amine and linker. Density functional theory calculations performed at the 6-31G(d,p) level revealed that the higher wavelength absorption contains a major contribution from the charge–transfer transition between the amine donor to the dicyanovinyl acceptor. The HOMO is mainly located on the triarylamine segment while the LUMO is spread over the dicyanovinyl. The fluorene based dyes exhibit lower thermal stability than their biphenyl analogues.

1. Introduction

Red-emitting dyes containing donor and acceptor moieties have received considerable attention over many years owing to their use in organic light-emitting diodes and photovoltaics [1,2]. Red-emitting dyes incorporating either low-band gap chromophores such as benzothiadiazole [3], thienopyrazine [4], maleimide [5] or fumaronitrile [6] and substituted with arylamines or polyacenes [7] have been described. Molecules containing polyaromatic segments tend to aggregate due to the facile π–π stacking of the planar segments which is detrimental for emission properties, though beneficial for charge transport characteristics [8]. In contrast, structures featuring donor–acceptor architecture inherit a strong dipole which triggers dipole–dipole interactions in both the solid state and polar solution [9].

For light-emitting devices, it is necessary to minimize the above mentioned intermolecular interactions in order to secure optimal emission. Several strategies have been reported for alleviating concentration quenching of dipolar compounds in the solid state. One method employs the doping of red-emitting materials in a suitable host [10], the success of this physical method relying upon the isolation of molecules and reduction of molecular contact. However, bifluorene [11] and fluorene [12] based dipolar compounds containing diarylamine donors and dicyanoethylene acceptors, which show potential as emitting materials for electroluminescent devices, resist dipolar interactions in the solid state. Moreover, diarylaminofluorene, dicyanoethylene and fullerene triads exhibit a prolonged charge separated state owing to the presence of dicyanovinyl group as electron-mediating bridge [13]. Among the triarylamine electron donors known to-date, fluorene based materials are attractive for their thermal, chemical and redox stability in addition to their excellent photoluminescence, electroluminescence and charge migration properties [14]. Combination of these properties makes them one of the most frequently employed chromophores in the design of materials suitable for electroluminescence and photovoltaic devices.

The present authors reported a series of diarylaminofluorene or diarylaminobiphenyl and cyanoacrylic acid conjugates which exhibited promising device performance parameters in dye-sensitized solar cells [15]. The absorption characteristics of the dyes were largely dependent on the nature of the bridging unit (fluorene or biphenyl) and the donor strength of the diarylamine segment tethered to the bridging segment [15]. As an extension to this work, a series of dicyanovinyl derivatives have been prepared to explore the differences in electronic properties arising from changes in acceptor segment. This paper concerns the synthesis and spectral, thermal and electrochemical characterisation of red dyes containing diarylaminobiphenyl or diarylaminofluorene electron donors

* Corresponding author. Tel.: +91 1332 285376; fax: +91 1332 286202.
E-mail address: krjt8fcy@iitr.ernet.in (K.R. Justin Thomas).

0143-7208/$ – see front matter © 2010 Elsevier Ltd. All rights reserved.
doi:10.1016/j.dyepig.2010.06.008

and dicyanovinyl electron acceptors. Correlation of the acceptor strength variation due to the dicyanovinyl and cyanoacrylic acid units with the absorption, emission and electrochemical properties were critically investigated.

2. Experimental

2.1. General

All reactions and manipulations were carried out under N_2 with the use of standard inert atmosphere and Schlenk techniques. Solvents were dried by standard procedures. Column chromatography purification was performed with the use of silica gel (230–400 mesh, Rankem, India) as the stationary phase in a column with 40 cm long and 3.0 cm diameter. The IR spectra were recorded on a THERMO Nicolet spectrometer. The ^{1}H and ^{13}C NMR spectra were measured with either a Bruker AMX500 or AMX400 spectrometer. Mass spectra were recorded on a JMS-700 double focusing mass spectrometer (JEOL, Tokyo, Japan). Electronic absorption spectra were obtained from either a Shimadzu spectrophotometer or Evolution UV–visible spectrophotometer. The fluorescence spectra were measured on a Shimadzu spectrofluorimeter. All the optical measurements were carried out using the freshly prepared dye solutions. Spin coated thin films were prepared from toluene solutions and used for the measurement of solid state photoluminescence. The TGA analyses were performed on a Perkin Elmer Pyris Diamond Analyzer using nitrogen as carrier gas and at a heating rate 10 °C/min.

Cyclic voltammetric experiments were performed with a CH Instruments 603C electrochemical analyzer. All the measurements were carried out at room temperature with a conventional three-electrode configuration consisting of a glassy carbon working electrode, a platinum wire auxiliary electrode, and a nonaqueous $Ag/AgNO_3$ acetonitrile reference electrode. The E_{ox} values were determined as $(E_p^a + E_p^c)/2$, where $E_p^a$and E_p^c are the anodic and cathodic peak potentials, respectively. The potentials are quoted against the ferrocene internal standard. Approximately 2.5×10^{-4} M acetonitrile solutions of the dyes were used in the electrochemical measurements, and the 0.1 M tetrabutylammonium hexafluorophosphate served as supporting electrolyte.

2.2. Synthesis

The dicyanovinyl derivatives of the aldehydes (**A1**–**A5**) [15] were obtained by following an identical procedure involving the Knoevenagel condensation of malononitrile with appropriate aldehyde. A representative procedure is illustrated below for **D1** and the remaining red dyes were obtained using the requisite aldehyde.

2.2.1. Synthesis of 2-((4′-(diphenylamino)biphenyl-4-yl)methylene) malononitrile(*D1*)

A 100 mL round bottom flask was charged with 4′-(diphenylamino)biphenyl-4-carbaldehyde (**A1**, 0.349 g, 1 mmol), malononitrile (0.099 g, 1.5 mmol), ethanol (10 mL) and a drop of piperidine. The mixture was heated under reflux for 8 h with protection from moisture. After the reaction was judged to be complete by TLC examination the mixture was cooled to 0 °C and the precipitate collected by filtration and washed well with cold methanol. Reddish orange solid, yield 0.302 g (76%); mp 135 °C. IR (KBr) ν: 2225 cm^{-1} ($\nu_{C\equiv N}$). ^{1}H NMR (400 MHz, $CDCl_3$) δ: 7.05–7.14 (m, 8H), 7.24–7.30 (m, 4H), 7.50 (d, J = 8.8 Hz, 2H), 7.69–7.72 (m, 3H), 7.94 (d, J = 8.4 Hz, 2H). ^{13}C NMR (125.770 MHz, $CDCl_3$) δ: 159.16, 149.05, 147.16, 131.65, 131.53, 129.58, 129.51, 129.23, 128.01, 127.10, 125.22, 123.90, 123.16, 122.70, 114.24, 113.15, 81.00. HR MS (ESI) m/z calcd. for $C_{28}H_{19}N_3$: 397.1579; Found: 397.1577.

2.2.2. Synthesis of 2-((4′-(naphthalen-2-yl(phenyl)amino)biphenyl) methylene)-malononitrile (*D2*)

D2 was synthesized from 4′-(naphthalen-1-yl(phenyl)amino) biphenyl-4-carbaldehyde (**A2**) by following the procedure described above for **D1** in 82% yield as red solid. mp 135 °C. IR (KBr) ν: 2223 cm^{-1}($\nu_{C\equiv N}$). ^{1}H NMR (400 MHz, $CDCl_3$) δ: 6.99–7.04 (m, 3H), 7.14 (dd, J = 8.4 Hz, 1.2 Hz, 2H), 7.22–7.26 (m, 2H), 7.34–7.39 (m, 3H), 7.44–7.50 (m, 4H), 7.66–7.70 (m, 3H), 7.80 (d, J = 8.4 Hz, 1H), 7.88–7.92 (m, 4H). ^{13}C NMR (125.770 MHz, $CDCl_3$) δ: 159.12, 149.59, 147.42, 146.88, 142.78, 135.37,131.59, 131.19, 130.56, 129.41, 129.04, 128.60, 127.95, 127.50, 127.14, 126.94, 126.74, 126.44, 126.38, 124.01, 123.29, 123.16, 120.54, 114.22, 113.11, 80.82, 53.48. HR MS (ESI) m/z calcd. for $C_{32}H_{21}N_3$: 447.1753; Found: 447.1734.

2.2.3. Synthesis of 2-((7-(diphenylamino)-9,9-diethyl-9H-fluoren-2 -yl)methylene)-malononitrile (*D3*)

D3 was obtained from 7-(diphenylamino)-9,9-diethyl-9*H*-fluorene-2-carbaldehyde (**A3**) in 84% yield by following the general procedure described above for **D1**. Red solid, mp 193 °C. IR (KBr) ν: 2222 cm^{-1} ($\nu_{C\equiv N}$). ^{1}H NMR (400 MHz, $CDCl_3$) δ: 0.35 (t, J = 4.8, 6H), 1.82–2.0(m, 4H), 7.01–7.08 (m, 4H), 7.11–7.13 (m, 4H), 7.24–7.29 (m, 4H), 7.58 (d, J = 8.4 Hz, 1H), 7.72 (d, J = 8.0, 1H), 7.74 (s, 1H), 7.81 (dd, J = 8.0 Hz J = 1.2 Hz, 1H), 7.87 (s, 1H). ^{13}C NMR (125.770 MHz, $CDCl_3$) δ: 159.87, 153.38, 151.07, 149.79, 148.66, 147.47, 133.56, 131.70, 129.48, 128.80, 124.88, 124.53, 123.65, 122.47, 122.12, 119.64, 117.46, 114.6, 113.67, 56.34, 32.40, 8.58. HR MS (ESI) m/z calcd. for $C_{33}H_2N_3$: 465.2205; Found: 465.2203.

2.2.4. Synthesis of 2-((9, 9-diethyl-7-(naphthalen-2-yl(phenyl) amino)-9H-fluoren-2-yl) methy-lene)malononitrile (*D4*)

D4 was derived from 9,9-diethyl-7-(naphthalen-1-yl(phenyl) amino)-9*H*-fluorene-2-carbaldehyde in 79% yield as red solid. mp 194 °C. IR (KBr) ν: 2224 cm^{-1} ($\nu_{C\equiv N}$). ^{1}H NMR (400 MHz, $CDCl_3$) δ: 0.28 (t, J = 7.2 Hz, 6H), 1.78–190 (m, 4H), 6.89–6.93 (m, 2H), 6.99 (t, J = 7.6 Hz, 1H), 7.11–7.13 (m, 2H), 7.22–7.25 (m, 4H), 7.28–7.33 (m, 2H), 7.41–7.53 (m, 3H), 7.62 (d, J = 8.0 Hz, 1H), 7.18 (s, 1H), 7.62–7.79 (m, 2H), 7.84–7.92 (m, 3H). ^{13}C NMR (125.770 MHz, $CDCl_3$) δ: 159.83, 153.41, 150.93, 150.50, 148.86, 147.88, 143.20, 135.36, 132.67, 131.73, 130.87, 129.39, 128.58, 127.11, 126.90, 126.48, 126.38, 126.27, 124.42, 124.12, 123.24, 123.02, 122.14, 120.38, 119.43, 115.11 114.70, 113.70, 78.90, 72.15, 56.27, 50.62, 32.38, 8.47. HR MS (ESI) m/z calcd. for $C_{37}H_{29}N_3$: 515.2361; Found: 515.2369.

2.2.5. Synthesis of 2-((5-(9,9-diethyl-7-(naphthalen-1-yl(phenyl) amino)-9H-fluoren-2-yl)-thiophen-2-yl) methylene)malononitrile (*D5*)

It was obtained from 5-(9,9-diethyl-7-(naphthalen-1-yl(phenyl) amino)-9*H*-fluoren-2-yl)thiophene-2-carbaldehyde in 81% yield as dark red solid. mp 244 °C. IR (KBr) ν: 2228 cm^{-1} ($\nu_{C\equiv N}$). ^{1}H NMR (400 MHz, $CDCl_3$) δ: 0.30 (t, J = 7.2, 6H), 1.55–1.86 (m, 2H), 1.92–1.99 (m, 2H), 6.91–7.00 (m, 3H), 7.08 (d, J = 6.0, 2H), 7.19–7.23 (m, 2H), 7.28–7.33 (m, 2H), 7.41–7.52 (m, 5H) 7.57–7.68 (m, 3H) 7.76 (d, J = 8.4 Hz, 2H), 7.86–7.90 (m, 2H). ^{13}C NMR (125.770 MHz, $CDCl_3$) δ: 158.02, 151.93, 151.06, 150.46, 149.17, 148.42, 144.24, 143.61, 140.34, 135.35, 133.99, 133.56, 130.93, 129.73, 129.24, 128.48, 126.92, 126.52, 126.34, 126.30, 126.16, 126.02, 124.30, 124.08, 122.49, 122.23, 121.01, 120.62, 119.56, 116.16, 114.49, 113.65, 75.55, 56.34, 32.62, 8.51. HR MS (ESI) m/z calcd. for $C_{41}H_{31}N_3S$: 597.2239; Found: 597.2252.

2.3. Theoretical calculations

For theoretical dipole moment and electronic vertical transition calculations, the structures of the dyes were optimized by applying DFT with the hybrid B3LYP functional and 6-31G (d,p) basis set. In

the case of fluorene derivatives, the 9-ethyl substituents were replaced with hydrogen atoms to minimize the computational time. With the optimized structure, the ground state dipole moments were calculated with the DFT (B3LYP) models and the 6-31G (d,p) basis set. The electronic transitions were calculated using time-dependent DFT (B3LYP) theory and the 6-31G (d,p) basis set. Even though the time-dependent DFT method less accurately describes the states with charge–transfer nature, the qualitative trends in the TDDFT results can still offer correct physical insight. At least 10 excited states were calculated for each molecule. For all the dyes, the first excited states were highly optically active as indicated by the larger oscillator strengths; consequently, it was used as basis in the elucidation of other states.

3. Results and discussion

3.1. Synthesis and characterization

The red dyes (Fig. 1) were prepared by treating the aldehydes with malononitrile in the presence of piperidine as catalyst in a Knoevenagel condensation reaction (Scheme 1). The aldehydes required for the synthesis were available from an earlier investigation [15]. The dyes were obtained in excellent yields (76–84%) and characterized by ^{1}H and ^{13}C NMR spectroscopy and high resolution mass spectrometry. The data were found to be consistent with the expected structures. The vinyl protons of the dicyanovinyl derivatives (**D1**–**D4**) are more shielded (7.63–7.72 ppm) when compared to those in the analogous cyanoacrylic acid derivatives (8.10–8.33 ppm) [15]. As the dicyanovinyl moiety is a stronger electron withdrawing moiety than the cyanoacrylic acid segment, the upfield shift observed for the dyes **D1**–**D4** is probably arising due to enhancement in electron density in the vinyl segment caused by the effective delocalization of electrons from the amine to dicyanovinyl unit. The dyes are orange or red in color and freely soluble in common solvents including dichloromethane, tetrahydrofuran, methanol, dimethylformamide and toluene. The dilute solutions of the dyes appear dark yellow and fluoresce in the orange to red region depending on the solvent polarity (*vide supra*).

3.2. Optical spectra

The electronic absorption spectra of the dyes were examined in different solvents to access their solution specific electronic properties. The absorption spectra recorded for the dyes in dichloromethane are displayed in Fig. 2 and the data are collected in Tables 1 and 2.

All the dyes exhibit two distinct absorption bands. One in the near-UV region around 307–311 nm which corresponds to the π–π^* transition localized at the aromatic segment, i.e., fluorene; and the other is a strong absorption in the visible region around 450–479 nm, which can be assigned to an intramolecular charge transfer (ICT) between the triarylamine donating unit and the dicyanovinyl accepting moiety [16]. The assignment of the high energy transition to charge–transfer is also supported by the fact that it is red-shifted (~50 nm) in the dye **D5** owing to the presence of more electron-rich conjugation due to the extra thiophene unit. The charge–transfer nature of the low energy transition is further confirmed by the solvent dependence witnessed for this band (*vide supra*). The broad absorption band in these compounds suggests a good electronic delocalization throughout the entire molecular system.

The spectra of the four new dyes are quite similar, but individual biphenyl based dyes **D1** and **D2** display 27 and 28 nm hypsochromic shifts respectively when equated to that of the fluorene based analogs **D3** and **D4**. This blue shift presumably arises from the nonplanar linkage in the biphenyl unit, which declines the efficient conjugation between the donor and acceptor segments. It is also possible that the twisting in the excited state hinders the donor–acceptor interaction in the biphenyl based dyes and as a result leads to an inefficient charge transition. More efficient charge polarization would lead to more pronounced solvation and stabilization of the corresponding state. Additionally, as the fluorene segment is more electron-rich than the biphenyl unit, it may boost the donor–acceptor interaction by supporting the donor strength of the amino group [17]. Within a category, there is no difference in absorption wavelength observed for the diphenylamine and 1-naphthylphenylamine donors (compare **D1** with **D2** and **D3** with **D4**). This may be possibly due to the effective electron withdrawing nature of the dicyanovinyl moiety. On the contrary, in the dyes with cyanoacrylic acid acceptors the diphenylamine based dyes exhibited red-shifted absorption when compared to that of 1-naphthylphenylamine containing dyes [15]. These elucidations are further supported by the following observations: (a) The biphenyl based dyes (**D1** and **D2**) possess comparatively lower molar extinction coefficients (27.3×10^3 M^{-1} cm^{-1} and 28.4×10^3 M^{-1} cm^{-1}) for the charge–transfer band than the fluorene based analogues (**D3** and **D4**) (37.3×10^3 M^{-1} cm^{-1} and 38.5×10^3 M^{-1} cm^{-1}) when recorded in dichloromethane. The decrease of extinction coefficient for the biphenyl dyes may be credited to the decrease in the co-planarity between the electron donor and the electron acceptor which would eventually lower the magnitude of the transition probability. (b) The thiophene containing dye (**D5**) displays bathochromism in the absorption profile when compared to the congener (**D4**). Insertion of thiophene in the conjugation pathway has been demonstrated to red-shift the absorption in several donor–acceptor compounds [18]. The charge–transfer bands are broadened and less intense for **D5** indicating a possible overlap of the multiple electronic transitions of different

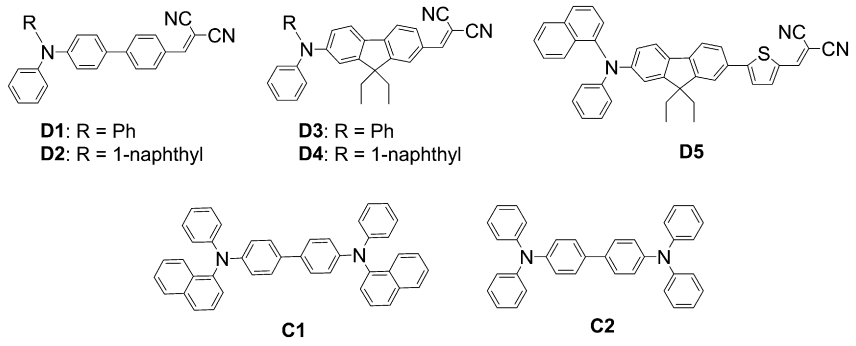

Fig. 1. Line drawings of the dyes (**D1**–**D5**) studied in this work.

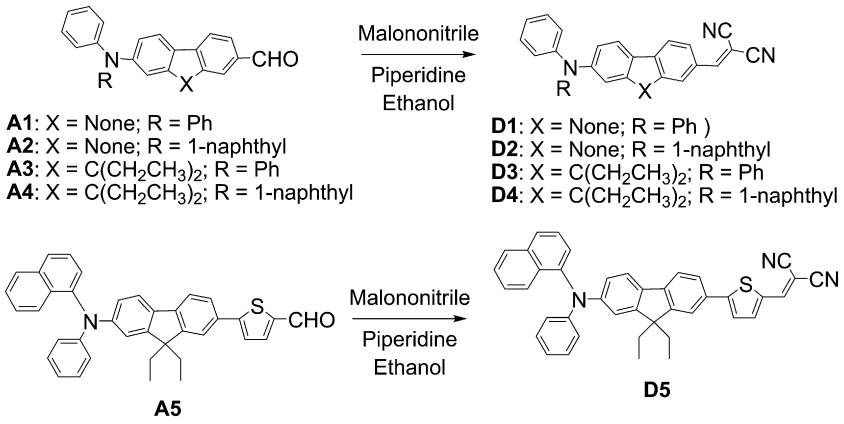

Scheme 1. Synthesis of the dyes (**D1**–**D5**).

origins. It is likely that the π–π* transition may share a wavelength region with the charge–transfer transition in the higher energy side which may remain unaltered during polarity change in the medium. Such an alternation is expected to result in increased intensity and a narrow band for non-polar solvents and lower intensity and a broader band for polar solvents (*vide supra*).

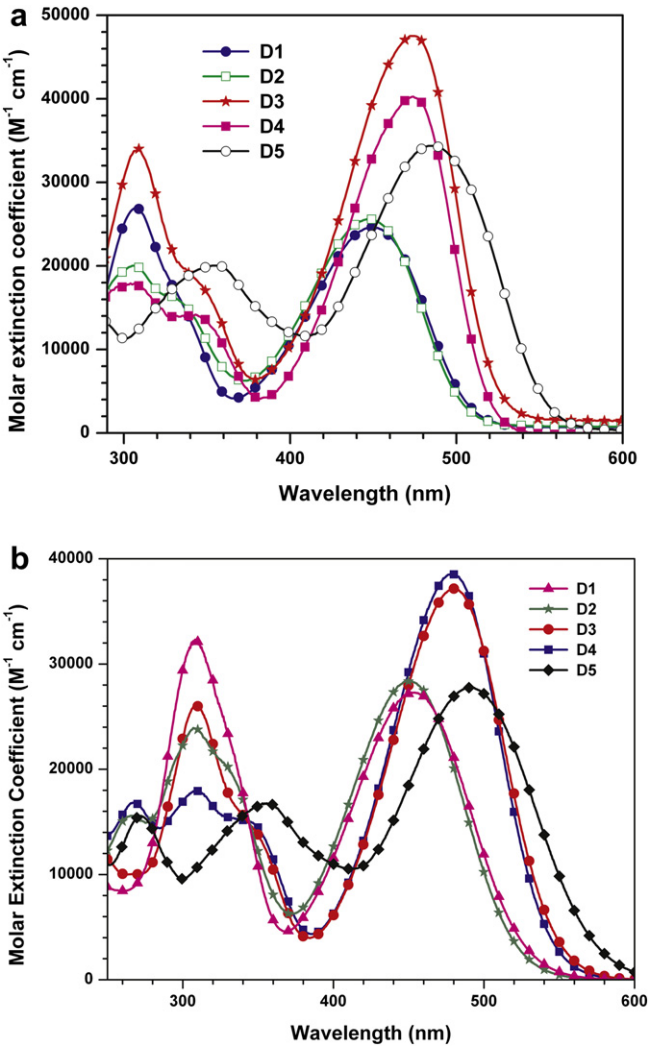

Fig. 2. Absorption spectra of the dyes (**D1**–**D5**) recorded in (a) toluene and (b) dichloromethane.

The effect of acceptor strength on absorption properties are clearly understood when the absorption spectra of the precursor amines (**B1**–**B4**) and aldehydes (**A1**–**A4**) are compared with the dicyanovinyl dyes. The absorption profile progressively shifts to the red region on going from the amines (**B1**–**B4**) to the dyes (**D1**–**D4**) *via* the intermediate aldehydes (**A1**–**A4**). The amines display absorption maxima below 350 nm while the aldehydes possess peaks above 350 nm (Fig. 3). If we presume that there is no charge–transfer transition present in the parent amines (**B1**–**B4**) then the red-shifted absorptions observed for the aldehydes (**A1**–**A4**) and the dyes (**D1**–**D4**) suggest a contribution of π–π* transition to the prominent band in these molecules (*vide supra*).

Another interesting aspect of these dyes is their solvatochromic behavior. The dyes exhibit negative solvatochromism for the charge–transfer transition from the amine donor to the dicyanovinyl acceptor moiety which occurs at longer wavelength. Representative absorption spectra of the dye **D3** recorded in selected solvents with varying dielectric constants are plotted in Fig. 4 and the relevant parameters collected in Table 2. An illustrative variation of absorption maxima *vs.* $E_T(30)$ parameter is plotted in Fig. 5 for the dye **D2**. The observed trend indicates that the dyes are efficiently solvated in the ground state in polar solvents. The ground state solvation is attributed to the efficient charge polarization present in the molecule triggered by the dipolar molecular structure. Such a stabilization of the ground state may lead to a widening of the band gap and lowering of the absorption wavelength in polar solvents. However, it must be mentioned that there is no linear correlation noticed for the absorption maximum with the solvent polarity as indicated by the plot of $E_T(30)$ parameter of the solvent against the absorption maxima (for example see Fig. 5). Larger deviation from linearity observed for the dyes in dichloromethane probably points to the fact that not only the dipolar interaction but

Table 1
Photophysical parameters of the dyes measured in toluene.

Dye	λ_{max}, nm (ε_{max}, M^{-1} cm^{-1} × 10^3)	λ_{em}, nm	Φ_F[a]	Stokes shift, cm^{-1}
D1	307 (26.9), 449.5 (24.6)	550.0	0.21	4065
D2	306 (20.0), 447.5 (25.6)	546.0	0.27	4031
D3	309 (34.0), 473.5 (47.5)	550.0	0.33	2938
D4	306.5 (17.9), 473.5 (40.3)	546.0	0.40	2804
D5	355 (20.0), 485.0 (34.4)	575.0	0.14	3227

[a] Quantum efficiency of the dyes were measured relative to Rhodamine-6G ($\Phi_F = 0.595$).

Table 2
Position of the charge transition observed for the dyes in different solvents.

Dye	λ_{max}, nm (ε_{max}, M^{-1} cm^{-1} × 10^3)					
	Toluene	THF	EA	DCM	DMF	ACN
D1	449.5 (24.6)	440.0 (13.2)	434.5 (23.0)	452.0 (27.3)	439.0 (12.9)	430.5 (21.9)
D2	447.5 (25.6)	439.0 (22.6)	433.0 (22.5)	450.0 (28.4)	437.5 (13.3)	430.5 (21.9)
D3	473.5 (47.5)	464.0 (26.9)	458.5 (33.9)	479.0 (37.3)	463.0 (25.7)	458.0 (37.0)
D4	473.5 (40.3)	466.0 (39.1)	460.0 (26.6)	478.0 (38.5)	465.5 (30.8)	459.0 (56.6)
D5	485.0 (34.4)	478.5 (32.1)	472.0 (37.6)	492.0 (27.8)	479.0 (31.1)	471.0 (40.9)

also the effective solvation of the dyes by the solvent influences the absorption profile. It may be inferred from the solvatochromic data that the hydrophobic toluene and bulkier dichloromethane are not effectively solvating the dyes while in the polar solvents such as acetonitrile and dimethylformamide pronounced solvation occurs.

3.3. Theoretical calculations

To determine the nature of the electronic transitions observed for the dyes, TDDFT/B3LYP calculations were performed on the dyes in the gas phase. The HOMO and LUMO orbitals predicted by the calculations were largely in keeping with the expectations and the electrochemical investigations (see below). The HOMO orbitals of the dyes were invariably located on the triarylamine unit and the LUMO orbitals spread over the dicyanovinyl acceptor segment (Fig. 6). The electronic transitions calculated at the 6-31G(d,p) level are displayed in Fig. 7 and the longer wavelength transitions are listed in Table 3. The longer wavelength transition calculated for the dyes are slightly red-shifted from the observed values for toluene. This also corroborates the involvement of solvent effects and the fact that in polar solvents, solvation stabilizes the molecules in the ground state and reduces the absorption wavelength. More-effective solvation might lead to a larger reduction in absorption wavelength. Since the red-shifted absorption peaks in the dyes are predicted to originate from the HOMO → LUMO transition they are assigned to the charge−transfer from the amine to dicyanovinyl group. Lower wavelength transitions (not listed in Table 3) are arising between π-type molecular orbitals located within the phenyl, naphthyl or fluorenyl segments. It must be noted that the trend which was observed between the biphenyl and fluorene based dyes are reversed in the TDDFT results. According to the calculations fluorene based dyes are hypothesized to show blue-shifted absorption when compared with the analogous biphenyl based dyes. It is possible that the more-effective solvation of the fluorene based dyes when compared to the biphenyl based dyes would have resulted in a red-shift in the absorption profile for solution measurements. The ground state dipole moments of the dyes are appreciably larger, when compared to the parent amines and the dipole moment significantly increased on introduction of aldehyde and dicyanovinyl moieties which is attributable to the enhancement of dipolar character.

3.4. Emission spectra

The emission properties of the dyes were examined in different solvents. Toluene was also used as solvent in the measurement of fluorescence spectra in order to avoid the complications that may arise due to the dipolar interactions and solvation effects. The emission spectra of the dyes recorded in toluene are displayed in Fig. 8 and the relevant parameters are collected in Table 1.

Irrespective of the difference in the nature of the amine and the conjugating segment present in the dyes, all the dyes with the exception of **D5** emit at approximately the same wavelength. For **D5**, the emission wavelength is red-shifted (~30 nm) when compared to the other dyes. The larger Stokes shift observed for the biphenyl based dyes (**D1** and **D2**) when compared to the fluorene containing dyes (**D3** and **D4**) is likely to arise due to the twisting occurring in the biphenyl conjugation on excitation while the rigidity of fluorene will forbid thermal rotational relaxation [19]. The emission colors of the dyes **D1**−**D4** in toluene may be described as green while it is orange for **D5**. In the solid state the emission is shifted to the higher wavelength. To ascertain the reason for this

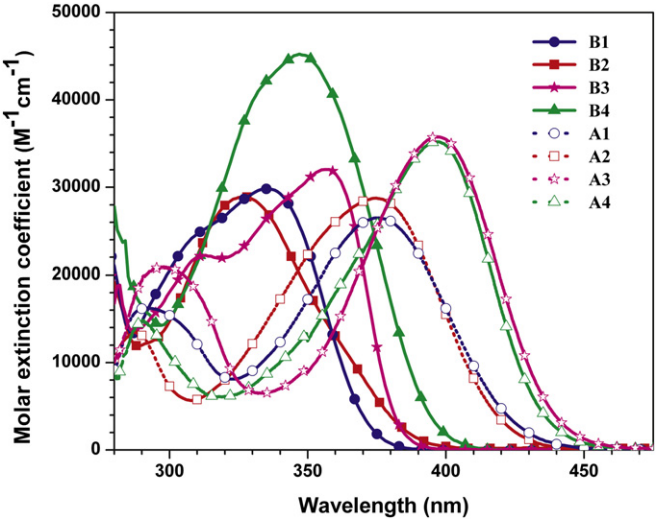

Fig. 3. Absorption spectra of the precursor amine and aldehydes recorded for dichloromethane solutions.

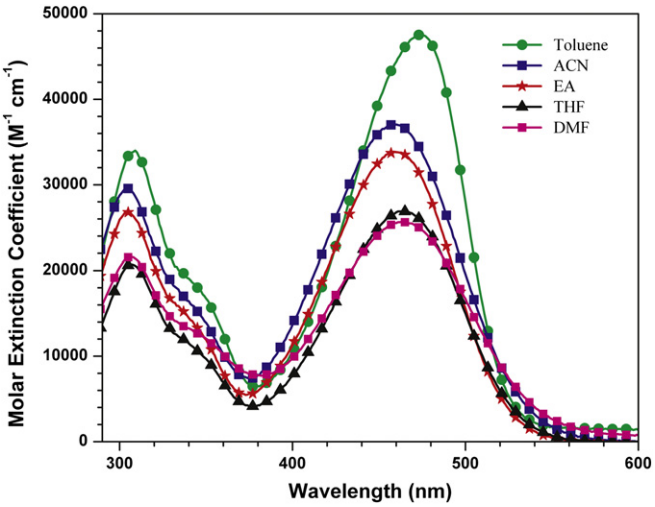

Fig. 4. Absorption spectra of the dye **D3** recorded in different solvents.

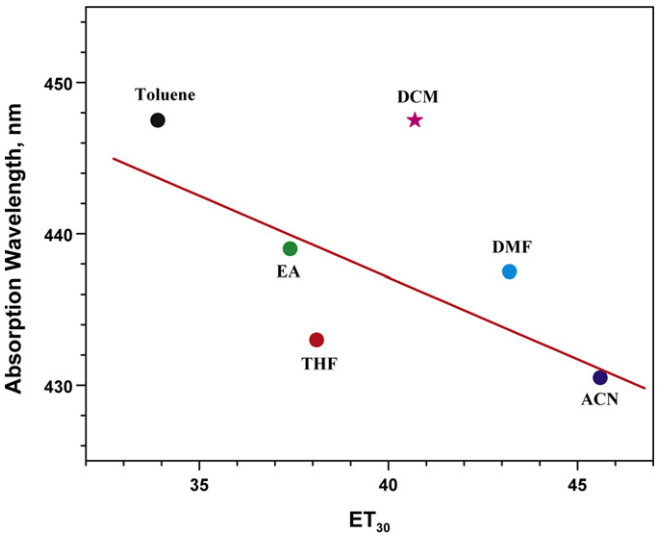

Fig. 5. Correlation of absorption maximum of **D2** with $E_T(30)$ values of the solvents used for measurement.

red-shift we have measured the emission spectra of the dyes in various solvents differing in dielectric constant (Table 4). In more polar solvents such as dimethylformamide and acetonitrile the dyes are non-emissive. However in dichloromethane and ethyl acetate a weak red-shifted fluorescence was observed. All these facts point the existence of pronounced dipolar interaction between the dipoles of the dyes and solvents. Consequently, the bathochromism observed for the film is assigned to the difference in dielectric constant [20] of the medium rather than the aggregation or stacking, which is quite unlikely in biphenyl systems due to inherent non-planarity.

3.5. Electrochemical properties

The bipolar character of the dyes was examined by using cyclic voltammetry. The electrochemical measurements were carried out in acetonitrile solution with 0.1 M tetrabutylammonium hexafluorophosphate as the electrolyte and at a scan rate 100 mV/s.

The cyclic voltammograms recorded for the dyes (**D1**–**D5**) in acetonitrile are displayed in Fig. 9. Except for **D2** all of the

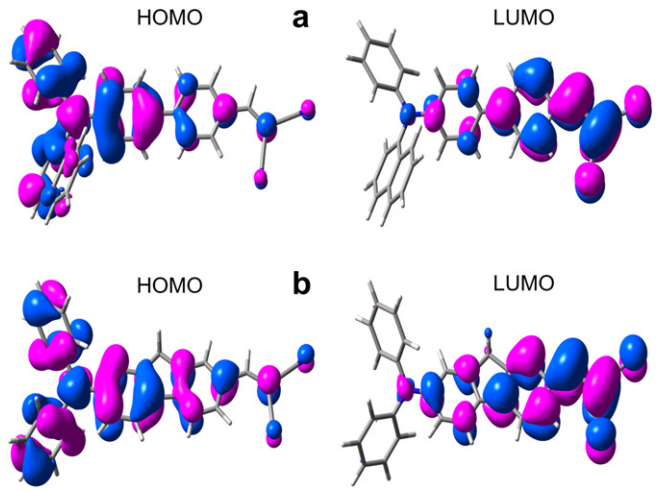

Fig. 6. Frontier molecular orbitals of the dyes (a) **D2** and (b) **D3**.

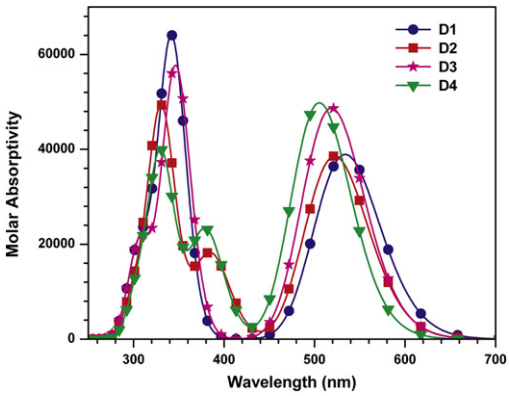

Fig. 7. Calculated absorption spectra of the dyes **D1**–**D5** in gaseous state.

compounds revealed a quasi-reversible oxidation couple attributable to the removal of an electron from the amine segment. The exact oxidation potential for **D2** dye was obtained from the differential pulse voltammetry. The negatively shifted oxidation (Table 5) observed for the fluorene based dyes is reasoned to the increased electron-rich character of the fluorene unit, which may increase the oxidation propensity of the amine unit. Insertion of the additional fluorene segment in the conjugation pathway has been demonstrated to significantly decrease the oxidation potential of the amines [21]. Also, substitution of the fluorene unit for the other aromatic units (phenyl, naphthyl) in the triarylamines has been reported to decrease the oxidation potential dramatically [22]. The oxidation potential of the present dyes is anodically shifted when compared to the parent triarylamines without electron accepting dicyanovinyl unit [15]. This clearly indicates the presence of an electronic interaction between the amine donor and the dicyanovinyl acceptor.

It is interesting to note that the oxidation potentials observed for **D3** and **D4** are more positive than that observed for **D5** which contain a thiophene unit between the fluorene and acceptor units. Cathodically shifted oxidation observed for **D5** is ascribed to the electron-rich character of the thiophene unit and decreased interaction between the amine donor and acceptor caused by the elongation in the conjugation [23]. Stronger interaction between the donor and acceptor will make the oxidation of the amine difficult. Even though no shift in absorption profile is noticed for the change in the diarylamine segment (compare **D1** with **D2** or **D3** with **D4**), it substantially affected the redox potential of the amino unit. Thus, the naphthylamine containing dyes displayed more positive oxidation potentials than that of the diphenylamine based dyes. This gives a route to design chromophores tunable in charge transport properties while retaining the optical character.

The orbital energies (Table 5) of the dyes were deduced by comparing the observed redox potentials with that of the internal

Table 3
TDDFT calculated dipole moments, frontier orbital energies, low energy vertical excitations and their assignments for the dyes.

Compd	HOMO, eV	LUMO, eV	Dipole Moment (Debye)	λ_{max}, nm	f	Assignment
B1	−5.031	−0.991	2.723	346.4	0.6537	HOMO → LUMO (90%)
A1	−5.128	−1.782	4.901	412.1	0.4643	HOMO → LUMO (93%)
D1	−5.318	−2.755	9.917	533.8	0.5375	HOMO → LUMO (91%)
D2	−5.347	−2.726	10.038	522.2	0.5323	HOMO → LUMO (91%)
D3	−5.282	−2.676	10.692	518.6	0.6724	HOMO → LUMO (88%)
D4	−5.308	−2.634	11.096	505.3	0.6878	HOMO → LUMO (88%)

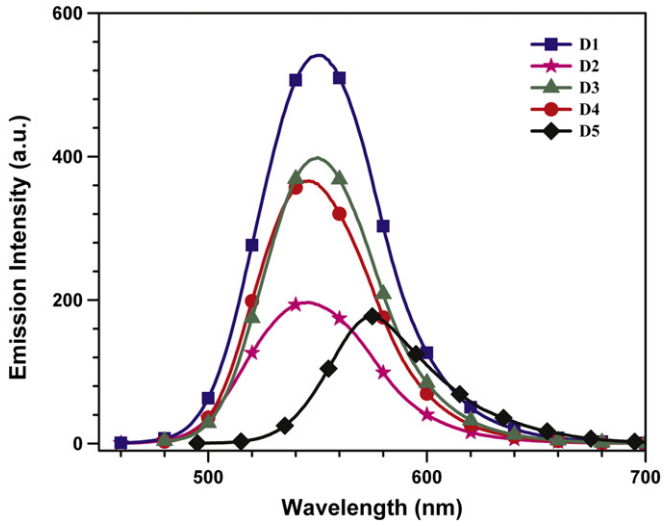

Fig. 8. Emission spectra of the dyes (**D1**–**D5**) recorded in toluene.

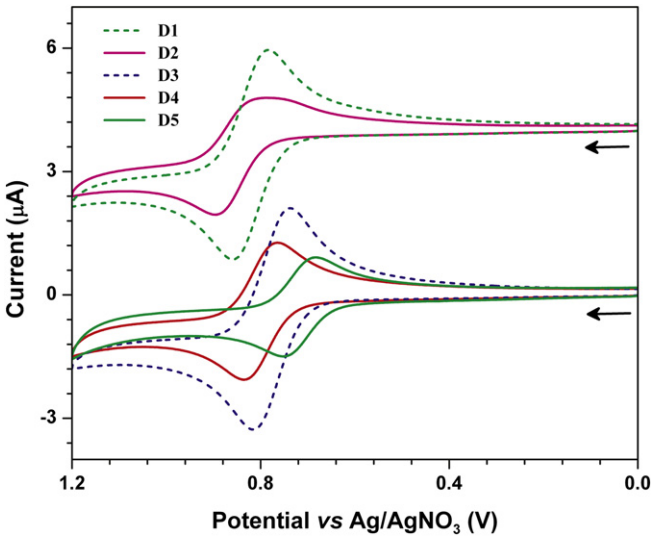

Fig. 9. Cyclic voltammograms recorded for the dyes (**D1**–**D5**) in acetonitrile. Supporting electrolyte: TBAHFP; scan rate: 0.1 V/sec.

standard and the absorption edge measured in the same solvent. The HOMO values were calculated from the oxidation potential by referencing to ferrocene which was used as internal standard as given below.

$$\text{HOMO} = E_{ox} + 4.8$$

While the LUMO was obtained from the optical band gap derived from the absorption edge using the equation:

$$\text{LUMO} = \text{HOMO} - E_{0-0}$$

The HOMO and LUMO values realized for the compounds suggest that they are potential to act as charge transporting emitters in a light-emitting device.

3.6. Thermal properties

The decomposition temperatures of the dyes **D1**–**D4** were measured by thermal gravimetric analysis (TGA) under a nitrogen atmosphere, with a heating rate of 10 °C/min. TGA indicated that these materials exhibit high decomposition temperatures (T_d). All the compounds exhibit a T_d value ranging from 400 to 432 °C (Table 6). The highest value is observed for **D2**, while **D3** shows the lowest in the series. The thermal decomposition temperatures of biphenyl based dyes (**D1** & **D2**) are higher than those containing fluorene chromophore (**D3** & **D4**) which is attributed to the fragile ethyl groups present in the molecule. Within the class, the dyes containing diphenylamine donor (**D1** & **D3**), display lower thermal decomposition temperature when compared with those possessing naphthylphenylamine donor (**D2** & **D4**). The presence of fused aromatic groups such as pyrene, carbazole and naphthalene has been demonstrated to increase the thermal stability of the organic functional materials [24]. For the same arguments, thermal stability difference observed between naphthyl and phenyl derivatives is assigned to the rigidity of naphthyl units. Additionally, the dyes also showed reasonable glass transition temperature (T_g) above 50 °C. The T_g did not differ very much between the biphenyl and fluorene dyes, however the amine unit played a significant role. The naphthylamine based dyes (**D2** and **D4**) exhibited higher T_g when compared to the analogous diphenylamine based ones (**D1** and **D3**). Enhancement of T_g due to the presence of naphthyl segments is observed earlier. For instance, the commonly employed hole-transporting material $N^4,N^{4'}$-di(naphthalen-1-yl)-$N^4,N^{4'}$-diphenyl-[1,1′-biphenyl]-4,4′-diamine (**C1**) shows higher T_g (95 °C) when compared to the analogous $N^4,N^4,N^{4'},N^{4'}$-tetraphenyl-[1,1′-biphenyl]-4,4′-diamine (**C2**) (70 °C) [25].

Table 4
Emission peak wavelengths of the dyes in different solvents.

Dye	λ_{em}, nm				Stokes Shift		
	Toluene	EA	DCM	Film	Toluene	EA	DCM
D1	550	588	613	616	4065	6008	5811
D2	546	580	525	614	4031	5853	3175
D3	550	581	612	631	2938	4599	4537
D4	546	578	603	597	2804	4438	4337
D5	575	633	612	666	3227	5389	3985

Table 5
Electrochemical data of the red dyes.

Compound	E_{ox} (ΔE_p), V[a]	HOMO, eV[b]	LUMO, eV[b]	$E_{0\text{-}0}$, eV	$E^*_{0\text{-}0}$, V[c]
D1	0.678	5.478	3.179	2.299	−0.99
D2	0.682	5.682	3.204	2.278	−0.97
D3	0.620	5.420	3.009	2.411	−1.16
D4	0.647	5.447	3.060	2.387	−1.11
D5	0.587	5.387	3.268	2.119	−0.90

[a] Measured for 2.0×10^{-5} M acetonitrile solutions at a scan rate of 0.1 V/s and 0.1 M tetrabutylammonium hexafluorophosphate (TBAHP) was used as supporting electrolyte.
[b] Deduced from the equations HOMO = E_{ox} + 4.8 and LUMO = HOMO − $E_{0\text{-}0}$.
[c] Excited state oxidation potential *vs* NHE.

Table 6
Thermal properties of dicyanovinyl derivatives.

Dye	T_m (°C)	T_{onset} (°C)	T_d (°C)	T_g (°C)
D1	135.0	340	406	52.0
D2	135.0	335	432	75.5
D3	193.0	330	400	58.0
D4	194.0	370	430	75.5
D5	244.0	338	431	97.0

4. Conclusions

In summary a series of red-emitting dicyanovinyl derivatives featuring biphenyl or fluorene conjugation and diphenylamino or naphthylphenylamino donor units have been synthesized. The electron withdrawing dicyanovinyl moiety is stronger electron withdrawing group than the cyanoacrylic acid unit and dictates the absorption properties of the dyes **D1**–**D4**. Electron withdrawing dicyanovinyl moiety dictates the absorption properties of the dyes and they behave as strong electron withdrawing group when compared to the cyanoacrylic acid unit. Due to this strong electron withdrawing character the difference in donor strength between the diphenylamine and naphthylphenylamine groups is not manifested in the absorption and fluorescence properties significantly. However, the electrochemical and thermal properties of the dyes are affected by the nature of the amine unit. Also, the dyes exhibit negative solvatochromism which indicate that the dyes display charge polarization in the ground state. Due to the promising properties such as reversible oxidation and red-shifted absorption, we believe that these materials may be efficiently used as charge transporting emitters in light-emitting diodes.

Acknowledgements

This work was supported by Department of Science and Technology, New Delhi (Grant No. SR/S1/OC-11/2007) and through an initiation grant by the Indian Institute of Technology Roorkee.

Appendix. Supplementary data

Absorption, ^{1}H, and ^{13}C NMR spectra and the thermogravimetric traces of the dyes are provided in the Supporting Information. Supplementary data associated with this article can be found in the online version, at doi:10.1016/j.dyepig.2010.06.008.

References

[1] (a) Reviews on various aspects of organic electroluminescence: Chen CT. Evolution of red organic light-emitting diodes: materials and devices. Chemistry of Materials 2004;16(23):4389–400;
(b) Kulkarni AP, Tonzola CJ, Babel A, Jenekhe SA. Electron transport materials for organic light-emitting diodes. Chemistry of Materials 2004;16(23):4556–73.

[2] (a) Briseno AL, Tseng RJ, Ling MM, Falcao EHL, Yang Y, Wudl F, et al. High-performance organic single-crystal transistors on flexible substrates. Advanced Materials 2006;18(17):2320–4;
(b) Yoon MH, Facchetti A, Stern CE, Marks TJ. Fluorocarbon-modified organic semiconductors: molecular architecture, electronic, and crystal structure tuning of arene-versus fluoroarene-thiophene oligomer thin-film properties. Journal of the American Chemical Society 2006;128(17):5792–801.

[3] Huang J, Qiao X, Xia Y, Zhu X, Ma D, Cao Y, et al. A dithienylbenzothiadiazole pure red molecular emitter with electron transport and exciton self-confinement for nondoped organic red-light-emitting diodes. Advanced Materials 2008;20(21):4172–4.

[4] (a) Mondal R, Miyaki N, Becerril HA, Norton JE, Parmer J, Mayer AC, et al. Synthesis of acenaphthyl and phenanthrene based fused-aromatic thienopyrazine co-polymers for photovoltaic and thin film transistor applications. Chemistry of Materials 2009;21(15):3618–28;
(b) Becerril HA, Miyaki N, Tang ML, Mondal R, Sun YS, Mayer AC, et al. Transistor and solar cell performance of donor–acceptor low bandgap copolymers bearing an acenaphtho[1,2-b]thieno[3,4-e]pyrazine (ACTP) motif. Journal of Materials Chemistry 2009;19(5):591–3;
(c) Nietfeld JP, Heth CL, Rasmussen SC. Poly(acenaphtho[1,2-b]thieno[3,4-e]pyrazine): a new low band gap conjugated polymer. Chemical Communications 2008;8:981–3.

[5] (a) Yeh TS, Chow TJ, Tsai SH, Chiu CW, Zhao CX. Electroluminescence of bisindolylmaleimide derivatives containing pentafluorophenyl substituents. Chemistry of Materials 2006;18(3):832–9;
(b) Yeh HC, Wu WC, Wen YS, Dai DC, Wang JK, Chen CT. Derivative of alpha, beta-dicyanostilbene: convenient precursor for the synthesis of diphenylmaleimide compounds, E-Z isomerization, crystal structure, and solid-state fluorescence. Journal of Organic Chemistry 2004;69(19):6455–62.

[6] Palayangoda SS, Cai X, Adhikari RM, Neckers DC. Carbazole-based donor–acceptor compounds: highly fluorescent organic nanoparticles. Organic Letters 2008;10(2):281–4.

[7] (a) Liu F, Xie LH, Tang C, Liang J, Chen QQ, Peng B, et al. Facile synthesis of spirocyclic aromatic Hydrocarbon derivatives based on o-Halobiaryl route and Domino reaction for Deep-blue organic semiconductors. Organic Letters 2009;11(17):3850–3;
(b) Su SJ, Chiba T, Takeda T, Kido J. Pyridine-containing triphenylbenzene derivatives with high electron mobility for highly efficient phosphorescent OLEDs. Advanced Materials 2008;20(11):2125–7;
(c) Wu JS, Pisula W, Mullen K. Graphenes as potential material for electronics. Chemical Reviews 2007;107(3):718–47.

[8] (a) Anthony JE. The larger acenes: versatile organic semiconductors. Angewandte Chemie-International Edition 2008;47(3):452–83;
(b) Ahmed E, Briseno AL, Xia Y, Jenekhe SA. High mobility single-crystal field-effect transistors from bisindoloquinoline semiconductors. Journal of the American Chemical Society 2008;130(4):1118–9.

[9] Gunbas GE, Durmus A, Toppare L. Could green be greener? Novel donor-acceptor-type electrochromic polymers: towards excellent neutral green materials with exceptional transmissive oxidized states for completion of RGB color spaces. Advanced Materials 2008;20(4):691–3.

[10] (a) Lee YT, Chiang CL, Chen CT. Solid-state highly fluorescent diphenylaminospirobifluorenylfumaronitrile red emitters for non-doped organic light-emitting diodes. Chemical Communications 2008;2:217–9;
(b) Ning ZJ, Chen Z, Zhang Q, Yan YL, Qian SX, Cao Y, et al. Aggregation-induced emission (AIE)-active starburst triarylamine fluorophores as potential non-doped red emitters for organic light-emitting diodes and Cl_2 gas chemodosimeter. advanced functional materials 2007;17(18):3799–807.

[11] Morel Y, Irimia A, Najechalski P, Kervella Y, Stephan O, Baldeck PL, et al. Two-photon absorption and optical power limiting of bifluorene molecule. Journal of Chemical Physics 2001;114(12):5391–6.

[12] Saragi TPI, Spehr T, Siebert A, Fuhrmann-Lieker T, Salbeck J. Spiro compounds for organic optoelectronics. Chemical Reviews 2007;107(4):1011–65.

[13] El-Khouly ME, Padmawar P, Araki Y, Verma S, Chiang YY, Ito O. Photoinduced processes in a tricomponent molecule consisting of diphenylaminofluorene-dicyanoethylene-methano[60]fullerene. Journal of Physical Chemistry A 2006;110(3):884–91.

[14] Thomas KRJ, Lin JT, Hsu YC, Ho KC. Organic dyes containing thienylfluorene conjugation for solar cells. Chemical Communications 2005;32:4098–100.

[15] Baheti A, Tyagi P, Thomas KRJ, Hsu YC, Lin JT. Simple triarylamine-based dyes containing fluorene and biphenyl linkers for efficient dye-sensitized solar cells. Journal of Physical Chemistry C 2009;113(20):8541–7.

[16] (a) Budy SM, Suresh S, Spraul BK, Smith Jr DW. High-temperature chromophores and perfluorocyclobutyl copolymers for electro-optic applications. Journal of Physical Chemistry C 2008;112(21):8099–104;
(b) Xia PF, Feng XJ, Lu J, Tsang SW, Movileanu R, Tao Y, et al. Donor-acceptor oligothiophenes as low optical gap chromophores for photovoltaic applications. Advanced Materials 2008;20(24):4810–2;
(c) Qin P, Zhu H, Edvinsson T, Boschloo G, Hagfeldt A, Sun L. Design of an organic chromophore for p-type dye-sensitized solar cells. Journal of the American Chemical Society 2008;130(27):8570–1.

[17] Hreha RD, George CP, Haldi A, Domercq B, Malagoli M, Barlow S, et al. 2,7-Bis (diarylamino)-9,9-dimethylfluorenes as hole-transport materials for organic light-emitting diodes. Advanced Functional Materials 2003;13(12):967–73.

[18] Thomas KRJ, Hsu YC, Lin JT, Lee KM, Ho KC, Lai CH, et al. 2,3-disubstituted thiophene-based organic dyes for solar cells. Chemistry of Materials 2008;20(5):1830–40.

[19] Peng ZK, Tao SL, Zhang XH, Tang JX, Lee CS, Lee ST. New fluorene derivatives for blue electroluminescent devices: influence of substituents on thermal properties, photoluminescence, and electroluminescence. Journal of Physical Chemistry C 2008;112(6):2165–9.

[20] Barto Jr RR, Frank CW. Near-infrared optical absorption behavior in high-beta nonlinear optical chromophore-polymer guest-host materials. 1. Continuum dielectric effects in polycarbonate hosts. Journal of Physical Chemistry B 2004;108(25):8702–15.

[21] (a) Lin JT, Chen PC, Yen YS, Hsu YC, Chou HH, Yeh MCP. Organic dyes containing furan moiety for high-performance dye-sensitized solar cells. Organic Letters 2009;11(1):97–100;
(b) Huang ST, Hsu YC, Yen YS, Chou HH, Lin JT, Chang CW, et al. Organic dyes containing a cyanovinyl entity in the spacer for solar cells applications. Journal of Physical Chemistry C 2008;112(49):19739–47;
(c) Thomas KRJ, Velusamy M, Lin JT, Chuen CH, Tao YT. Chromophore-labeled quinoxaline derivatives as efficient electroluminescent materials. Chemistry of Materials 2005;17(7):1860–6.

[22] (a) Li ZH, Wong MS, Fukutani H, Tao Y. Synthesis and light-emitting properties of bipolar oligofluorenes containing triarylamine and 1,2,4-triazole moieties. Organic Letters 2006;8(19):4271–4;
(b) Thomas KRJ, Lin JT, Tao YT, Chuen CH. Green and yellow electroluminescent dipolar carbazole derivatives: features and benefits of electron-withdrawing segments. Chemistry of Materials 2002;14(9):3852–9.

[23] Thomas KRJ, Lin JT, Tao YT, Ko CW. Quinoxalines incorporating triarylamines: potential electroluminescent materials with tunable emission characteristics. Chemistry of Materials 2002;14(3):1354–61.

[24] (a) Adhikari RM, Mondal R, Shah BK, Neckers DC. Synthesis and photophysical properties of carbazole-based blue light-emitting dendrimers. Journal of

Organic Chemistry 2007;72(13):4727–32;
(b) Mikroyannidis JA, Fenenko L, Adachi C. Synthesis and photophysical characteristics of 2,7-fluorenevinylene-based trimers and their electroluminescence. Journal of Physical Chemistry B 2006;110(41):20317–26;
(c) Thomas KRJ, Velusamy M, Lin JT, Tao YT, Chuen CH. Cyanocarbazole derivatives for high-performance electroluminescent devices. Advanced Functional Materials 2004;13(4):387–92;
(d) Thomas KRJ, Lin JT, Tao YT, Ko CW. Light-emitting carbazole derivatives: potential electroluminescent materials. Journal of the American Chemical Society 2001;123(38):9404–11.
[25] Saragi TPI, Fuhrmann-Lieker T, Salbeck J. Comparison of charge-carrier transport in thin films of spiro-linked compounds and their corresponding parent compounds. Advanced Functional Materials 2006;16(7):966–74.